Separation & Purification Reviews
Publication details, including instructions for authors and subscription information:
http://www.informaworld.com/smpp/title~content=t713597294

Separation of Isotopes in the Thermal Diffusion Column

W. M. Rutherford[a]
[a] Monsanto Research Corporation, Mound Laboratory, Miamisburg, Ohio

To cite this Article Rutherford, W. M.(1975) 'Separation of Isotopes in the Thermal Diffusion Column', Separation & Purification Reviews, 4: 2, 305 — 350
To link to this Article: DOI: 10.1080/03602547508066043
URL: http://dx.doi.org/10.1080/03602547508066043

SEPARATION AND PURIFICATION METHODS, 4(2), 305-350 (1975)

SEPARATION OF ISOTOPES IN THE THERMAL DIFFUSION COLUMN

W. M. Rutherford
Monsanto Research Corporation, Mound Laboratory, Miamisburg, Ohio 45342*

I. INTRODUCTION

Gas, liquid and solid mixtures undergo a slight demixing in the presence of a temperature difference. This phenomenon, known as thermal diffusion, is illustrated in Figure 1 for the isotopes of neon in the gas phase and for isotopically substituted carbon disulfide in the liquid phase. The separation effect, which is quite small even for relatively large temperature differences, was of no practical significance prior to the invention by Clusius and Dickel of the thermogravitational thermal diffusion column in 1938[1]. In the thermal diffusion column (Figure 2) the fluid is confined between closely spaced vertical walls maintained at different temperatures. A convection current is set up with the fluid rising along the hot wall and descending along the cold wall. Thermal diffusion takes place in the horizontal direction. The combined effects of vertical countercurrent thermogravitational circulation and horizontal thermal diffusion lead to large separations in the vertical direction. The equivalent of several hundred separ-

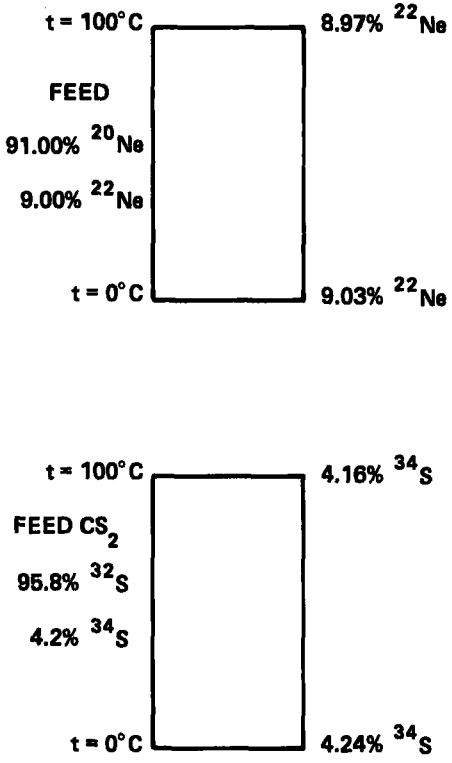

FIGURE 1

The elementary thermal diffusion effect in gas and liquid phases.

ation stages can be obtained in apparatus no more than a few meters in length.

Since its invention the thermal diffusion column has found numerous applications to special separations involving small quantities of material. The column has been used with particular success for the separation of gram quantities of isotopes in the gas phase. It provides a means whereby important needs for relatively minor amounts of material can be satisfied with

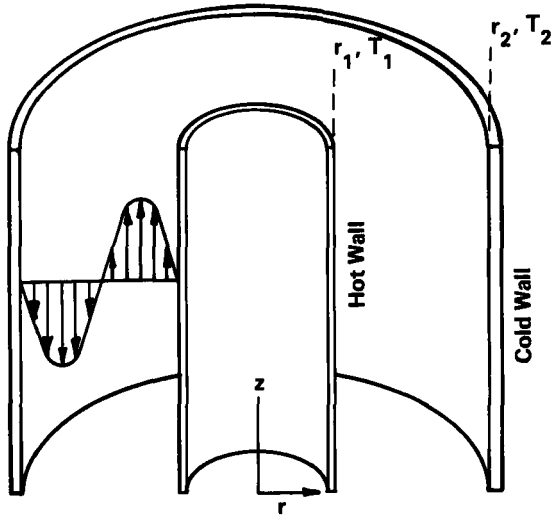

FIGURE 2

The cylindrical thermal diffusion column.

a minimal capital investment in simple equipment and minimal operating costs.

Some typical applications of isotopes separated by thermal diffusion are the following: ^{86}Kr as a fill gas for spectral lamps for wavelength standards; ^{38}Ar as a spike, or carrier, in the potassium-argon method for establishing geological times; ^{124}Xe as a target material for the nuclear reactor production of radioactive ^{125}I; enriched Kr and Xe isotopes for tracing fuel element failures in fast breeder reactors; and high enrichment of ^{13}C for multiple labeling of biologically and environmentally important tracer materials.

The thermal diffusion column has also found use as a quantitative enrichment technique in the determination of low levels of natural radionuclides. It has been used in carbon-14

dating[2], low level tritium measurements[3,4], and in the determination of atmospheric levels of ^{37}Ar.[4]

Many of the first research scale separations of isotopes in high purity were accomplished by Clusius and coworkers at Zurich[6]. A list of these and other separations is given as Table I[7]. The Clusius thermal diffusion columns were water cooled glass tubes, with an electrically heated platinum alloy wire hung along the axis as the hot wall. Typically, several of these columns were connected in series to obtain the effective length needed for a particular separation.

TABLE I

Stable Isotope Enrichment by Gas Phase Thermal Diffusion

Year	Isotope	% Purity
1939	Chlorine-35	99.4
1939	Chlorine-37	99.6
1942	Krypton-84	98.3
1942	Krypton-86	99.5
1950	Neon-20	99.95
1950	Nitrogen-15	99.8
1953	Carbon-13	99.8
1955	Xenon-136	99.0
1956	Neon-21	99.6
1959	Oxygen-18	99.7
1959	Argon-38	99.98
1960	Neon-22	99.92
1962	Argon-36	99.99
1968	Oxygen-16	99.98
1971	Xenon-131	60
1971	Argon-40	99.98
1972	Xenon-124	60
1972	Krypton-78	50
1973	Krypton-82	70
1973	Krypton-83	70
1973	Xenon-129	80

Some exceedingly difficult separations were accomplished with this type of apparatus, including the purification of the rare middle isotopes of neon and argon, ^{21}Ne[8] and ^{38}Ar.[9]

Thermal diffusion is now being used at several locations for the routine separation of a wide variety of isotopes. Although the Clusius-type column is used for some of this work, most of it is being done with all metal columns using commercially available tubular electric heaters for the hot wall[10]. Depending upon the difficulty of the separation, these columns are used in series - parallel cascades of from 4 to 24 columns.

The theory of the thermal diffusion column was developed in nearly complete form shortly after its invention. In 1939 Furry, Jones and Onsager (FJO) derived the basic equations describing the behavior of the cylindrical thermal diffusion column[11,12]. The FJO theory, which took into account the variation with temperature of the physical properties of the gaseous mixture and the cylindrical geometry of the column, was found to give a satisfactory qualitative description of the separation process. From the quantitative standpoint, however, the theory was less successful[13]. The discrepancies were generally attributed to deficiencies in the theory; however, it was recognized that imperfections in the experimental apparatus were important. In addition, measurements of the thermal diffusion factor, which is the measure of the elementary effect, were scarce at that time and of dubious accuracy.

Within the last few years the author and coworkers have undertaken a systematic investigation of the behavior of the thermal diffusion column and the extent to which that behavior can be predicted from theory[14-19]. The results have shown unequivocally that the FJO theory predicts the separation of heavy isotopes in precisely constructed thermal diffusion

columns within experimental accuracy. With minor modifications the theory also correctly predicts the separation of light isotopic mixtures such as ^{3}He-^{4}He.[20]

The successful verification of the column theory is due in no small measure to several concurrent developments including: improved understanding of intermolecular forces in dilute gases leading to better predictions of physical properties; availability of high precision, wide range viscosity data; development and application of the trennschaukel technique for accurate measurements of isotopic thermal diffusion factors; and the availability of high speed digital computers to facilitate integration of the FJO expressions for the column transport coefficients.

This review will be restricted to the theory and observed behavior of gas phase thermal diffusion columns as individual separation units. It will cover isotopic separations in noble gas systems and in gas phase systems of simple, polyatomic, isotopically substituted compounds. It will not cover work on isotopic separations in the liquid phase, nor will it cover the theoretical and experimental aspects of multiple column cascades. The theory of cascades of large numbers of interconnected separation units is a separate and rather large subject. The results of cascade theory are general and can be applied to any separation technique, including thermal diffusion.

No attempt will be made in this review to present a broad, inclusive picture of the work that has been reported in the literature on gas phase thermal diffusion. For this the reader is referred to the several very good bibliographies on thermal diffusion[21-23], and the 1969 review of Vasaru, et al[24]. Instead,

emphasis will be placed on the author's own work which has represented an effort to develop a systematic approach to the problem of predicting and evaluating the performance of gas phase thermal diffusion columns.

II. THEORY OF THE THERMAL DIFFUSION COLUMN

The discussion which follows pertains to the separation of a binary mixture in an ideal cylindrical thermal diffusion column. The theory was originally developed to describe the separation of light isotopic mixtures in the gas phase[20]; however, the results are general and can be applied to nonisotopic mixtures and to liquid systems. For isotopic mixtures of high atomic weight the results are the same as those of the original FJO theory.

In the derivation given in detail in Reference 20 the following assumptions are made:

1. The binary fluid mixture is confined in the annular space between two vertical, concentric right circular cylinders (Figure 2). The inner cylinder, of radius r_1 is at a uniform temperature, T_1; the outer cylinder, of radius r_2 is at a uniform temperature, T_2.
2. The convective circulation velocity, the temperature distribution, and the concentration are independent of the angular coordinate.
3. There is a small net mass flow σ in the positive z direction. The flow may be considered to result from the removal of a single product stream from the end of the column. The superficial velocity corresponding to this flow is negligible relative to the maximum velocity of the convective circulation.

4. The change in concentration in the radial direction is small.
5. The vertical concentration gradient is small; hence, terms involving derivatives of the density and the velocity with respect to the vertical coordinate can be neglected.

In the presence of temperature and concentration gradients, and of convection, the mass flux, $\vec{J}_1$, of component 1 of a binary mixture is given by

$$\vec{J}_1 = -D_{12}\rho(\vec{\nabla}w_1 - \alpha_T w_1 w_2 \vec{\nabla}\ell n\ T) + w_1\rho\vec{v}, \qquad (1)$$

where w_1 and w_2 are the mass fractions of the two components, $\vec{v}$ is the local mass average velocity, ρ is the mass density, and D_{12} is the mutual diffusion coefficient. The quantity α_T is the thermal diffusion factor defined in a way such that component 1 migrates in the direction of the temperature gradient, or toward the hot wall.

It should be noted here that Furry, Jones and Onsager[11,12] used as their starting point an equation of the same form for the molar flux in terms of mole fractions and, implicitly, the molar average velocity. The solution of the associated viscous flow problem, however, yields the mass average velocity; hence, the FJO theory applies only to mixtures for which the difference between these velocities can be ignored, e.g., to heavy isotopic mixtures.

Equation 1 can be used to derive the following equation for the transport, τ_1, of component 1 along the z direction of the column:

$$\tau_1 = Hw_1w_2 - (K_c+K_d)(dw_1/dz) + \sigma w_1. \qquad (2)$$

The quantities H, K_c, and K_d represent the following integrals which result from the derivation:

$$H = 2\pi \int_{T_2}^{T_1} \frac{\alpha_T G(T)}{T}\, dT, \tag{3}$$

$$K_c = \frac{2\pi}{Q} \int_{T_2}^{T_1} \frac{\lambda G^2(T)}{D_{12}\rho}\, dT, \tag{4}$$

$$K_d = \frac{2\pi}{Q} \int_{T_2}^{T_1} \lambda D_{12} \rho r^2\, dT. \tag{5}$$

The quantity H is generally referred to as the initial transport coefficient, and the quantities K_c and K_d are called the convective and diffusive remixing coefficients. In the above equations λ is the thermal conductivity, and $2\pi Q$ is the radial heat flow per unit length.

The quantity G is a function of the thermal convection rate and is given by

$$G(r) = \int_{r_1}^{r} \rho v r dr, \tag{6}$$

where $v = v_z$ is the vertical velocity[25]. Consideration of the thermogravitational viscous flow problem yields G as the solution of the fourth order differential equation,

$$Q^3 \frac{d}{dT} \frac{1}{r^2\lambda} \frac{d}{dT} \frac{\eta}{\lambda} \frac{d}{dT} \frac{1}{\rho\lambda r^2} \frac{dG}{dT} = -g \frac{d\rho}{dT}, \tag{7}$$

where g is the acceleration of gravity and the following boundary conditions apply:

$$G(T_1) = G(T_2) = \left(\frac{dG}{dT}\right)_{T=T_1} = \left(\frac{dG}{dT}\right)_{T=T_2} = 0. \tag{8}$$

The above results (except for the definition of G) are essentially the same as those given in the original work of Furry, Jones and Onsager; however, the mole fractions of the FJO theory have now been replaced by mass fractions, and the theory is no longer restricted to heavy isotopic mixtures.

Solutions of the Binary Transport Equation

In a column operated at total reflux and at the steady state σ and τ_1 are both equal to zero. Under these conditions the transport equation can be integrated to yield

$$\ln q = \frac{HL}{K_c+K_d}, \tag{9}$$

where L is the length of the column section and q, the separation factor is defined by

$$q = \frac{w_{1T}w_{2B}}{w_{1B}w_{2T}}. \tag{10}$$

The subscripts T and B refer to the top and bottom of the column section, respectively.

From Equation 7 it can be shown that the quantity G is proportional to the square of the density; hence, for an ideal gas G is proportional to p^2, where p is the pressure. Thus the transport coefficients H and K_c can be written as

$$H = H'p^2, \tag{11}$$

and

$$K_c = K_c'p^4, \tag{12}$$

where H' and K_c' are independent of pressure. (The coefficient K_d is independent of pressure.)

The separation factor at total reflux then becomes

$$\ln q = H'p^2/(K_c'p^4 + K_d). \tag{13}$$

This function reaches a sharp maximum at a pressure p_1 such that

$$K_c = K_c'p_1^4 = K_d. \tag{14}$$

If a product stream is removed from the top of the column section at a rate σ, then at the steady state

$$\tau_1 = \sigma w_{1T}, \tag{15}$$

and Equation 2 can be integrated to give the following:

$$\tanh\left(\frac{bY}{2}\right) = \frac{b(w_{1T}-w_{1B})}{w_{1T}+w_{1B}-(\sigma/H)(w_{1T}-w_{1B})-2w_{1T}w_{1B}}, \qquad (16)$$

where b is given by

$$b = \{[1+(\sigma/H)^2]-4\sigma w_{1T}/H\}^{\frac{1}{2}}, \qquad (17)$$

and $Y = HL/(K_c+K_d)$. In this case the integration has been performed over a column segment of length L starting from a product withdrawal point at the end of the column.

The performance of a complete separation unit comprising a column with stripping and enriching sections, as shown in Figure 3, can be calculated using the above solution. Each section is calculated separately. The upper section is treated as an enriching section for component 1 and the lower as an

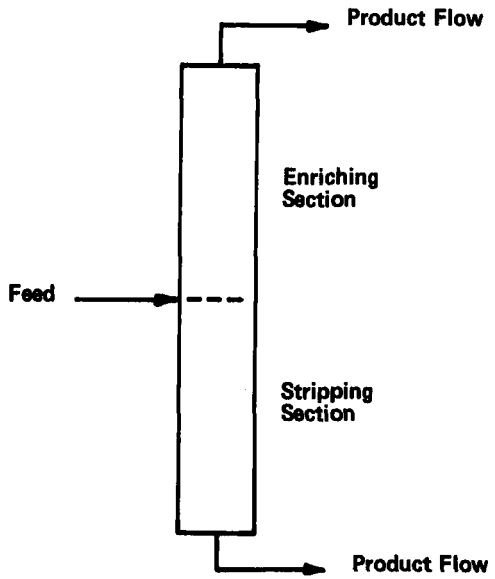

FIGURE 3

A complete thermal diffusion separation unit.

enriching section for component 2. A trial and error procedure is required to obtain values of the dependent variables (flows and/or concentrations) such that the material balance is satisfied. This requires that the same concentration be obtained at the feed point by calculating toward the feed point from either direction. (In general this composition is not the same as the feed composition.)

Transient Behavior of the Column

The differential equation which describes the transient behavior of the thermal diffusion column for a binary mixture can be obtained from the equation of continuity for component 1 along the z axis. Thus,

$$\frac{\partial w_1}{\partial t} = \frac{-1}{\mu} \frac{\partial \tau_1}{\partial z}, \tag{18}$$

where t is the time and μ is the mass holdup per unit length.

Substitution from Equation 2 yields the following result for the concentration in terms of the transport coefficients:

$$\mu \frac{\partial w_1}{\partial t} = H[1-2w_1 + \sigma] \frac{\partial w_1}{\partial z} + K \frac{\partial^2 w_1}{\partial z^2}, \tag{19}$$

where $K = K_c + K_d$.

Solutions of Equation 19 for $\sigma = 0$ and $w_1 \ll 1$ were given by Bardeen[26,27], and exact general solutions were given by Majumdar[28]. These solutions are for the case of the column with no reservoirs and for the case of the column with one infinite reservoir at one end and no reservoir at the other.

The Majumdar solutions are less generally useful than one might suppose. First, they require machine computation of the sums of two series for each time and position point; and second, experimental configurations seldom coincide with the mass distributions assumed for the derivations. Numerical solutions of Equation 19 by finite difference methods are not difficult,

and they can be accomplished for arbitrary mass distribution with relatively little investment in computing time for most problems.

This will be discussed in more detail in connection with multicomponent systems.

The Transport Equation for Multicomponent Systems

The equation analogous to Equation 1 for the mass flux of component i in a system of n components is

$$\vec{J}_i = -D\rho\left(\vec{\nabla}w_i - w_i\sum_{j}^{n-1}\alpha_{ij}w_j\vec{\nabla}\ell nT\right) + w_i\rho\vec{v} \qquad (20)$$

where α_{ij} is the thermal diffusion factor of the ijth pair and it has been assumed that $D_{ij} = D_{ii} = D_{jj} = D$. By carrying out the derivation in a way analogous to that for the binary system, one arrives at the following equation for the transport of component i of an n-component system:

$$\tau_i = w_i\sum_{j}^{n-1}H_{ij}w_j - K\frac{dw_i}{dz} + \sigma w_i \qquad (21)$$

The initial transport coefficient H_{ij} is given by

$$H_{ij} = 2\pi\int_{T_2}^{T_1}\frac{\alpha_{ij}G(T)}{T}\,dT, \qquad (22)$$

and the other transport coefficients are the same as those for the binary case.

For isotopic systems[29]

$$\alpha_{ij} = \alpha_o\left(\frac{M_i - M_j}{M_i + M_j}\right) \simeq \alpha_o\left(\frac{M_i - M_j}{2\bar{M}}\right), \qquad (23)$$

where α_o, the reduced thermal diffusion factor, is the same for all isotopic pairs, and $\bar{M}$ is the average molecular or atomic weight of the gas.

For computational purposes it is convenient to introduce a reduced initial transport coefficient, H_o, defined by

$$H_o = H_{ij}\left(\frac{M_i+M_j}{M_i-M_j}\right). \tag{24}$$

With this substitution Equation 21 becomes

$$\tau_i = H_o w_i \sum_{j}^{n-1} m_{ij} w_j - K\frac{dw_i}{dz} + \sigma w_i, \tag{25}$$

where

$$m_{ij} = \frac{M_i-M_j}{M_i+M_j}.$$

Solutions of the Multicomponent Transport Equation

At total reflux and at the steady state Equation 25 can be integrated to give

$$\ln q_{ij} = \frac{H_o m_{ij} L}{K}, \tag{26}$$

where q_{ij} is the separation factor between components i and j defined as in Equation 10 for a binary system.

If the column is not at total reflux, the problem is considerably more complicated. Steady state solutions of Equation 25 for the case of nonzero net flow ($\sigma \neq 0$) cannot be obtained in closed form for systems of more than two components. In general they must be found by numerical techniques. If the composition is known at one end of the column, then a straightforward application of the Runge-Kutta method suffices to find the concentration at any other point in the system.

If, however, boundary conditions for the problem are imposed in the form of material balances over a known feed stream and two product streams of unknown composition, then the problem becomes much more difficult. As in the analogous binary case, it is necessary to adjust the composition of one of the product streams until the calculated composition profile satisfies the material balance.

A full discussion of the numerical techniques involved in solving such problems is beyond the scope of this review. The

Newton-Raphson method using finite difference derivatives is quite useful for adjustment of the composition; however, a variety of frustrating numerical difficulties are often encountered, and great care must be used in choosing the form of the iteration variables and the form in which the associated deviations from the boundary conditions are expressed. The author has found no single set of techniques to be adequate for solving all problems.

Transient Behavior in Multicomponent Separations

The transient behavior of a column separating a multicomponent isotopic mixture is given by a set of nonlinear partial differential equations which can be obtained in a manner analogous to the binary case. Thus,

$$\frac{\partial w_i}{\partial t} = -\frac{1}{\mu}\frac{\partial \tau_i}{\partial z} . \tag{27}$$

Equation 27 can be expressed in terms of finite differences as

$$w_{i,m,k+1} = w_{i,m,k} + \frac{(\tau_{i,m,k}-\tau_{i,m-1,k})\Delta t}{\mu(z_m-z_{m-1})} , \tag{28}$$

where the index k refers to the time step and the index m refers to the distance step along the z direction. According to Equation 25

$$\tau_{i,m,k} = H_o\left[\bar{w}_{i,m,k}\sum_j m_{ij}\bar{w}_{j,m,k} - \frac{w_{i,m,k}-w_{i,m-1,k}}{Y_m-Y_{m-1}}\right] + \sigma\bar{w}_{i,m,k}, \tag{29}$$

where

$$\bar{w}_{i,m,k} = (w_{i,m,k} + w_{i,m-1,k})/2, \tag{30}$$

and

$$Y_m = \frac{H_o z_m}{K} . \tag{31}$$

The above equations can readily be stepped forward in time, provided that the time interval is appropriately chosen to

assure stability in the calculation. Unfortunately the maximum stable time interval, which is roughly proportional to the ratio $\mu\Delta z/H_o$, is quite short for most practical problems. Although useful solutions can be obtained, an inordinate amount of computer time is required to obtain them.

A different approximation to Equation 27 was developed in order to circumvent this problem. The transport during the kth time interval is taken to be the average of the transport at the beginning of the interval, $\tau_{i,m,k}$ and the transport at the end of the interval, $\tau_{i,m,k+1}$. Thus,

$$w_{i,m,k+1} = w_{i,m,k} + \frac{\Delta t}{\mu(z_m - z_{m-1})} \left[\frac{(\tau_{i,m,k} + \tau_{i,m,k+1})}{2} - \frac{(\tau_{i,m-1,k} + \tau_{i,m-1,k+1})}{2} \right], \quad (32)$$

where $\tau_{i,m,k}$ is given by Equation 29.

The system of equations given by 29 through 32 cannot be solved explicitly for the $w_{i,m,k+1}$, however, the equations can be reduced to a set of tridiagonal equations for each component, so that

$$Aw_{i,m-1,k+1} + Bw_{i,m,k+1} + Cw_{i,m+1,k+1} = D_{i,m}. \quad (33)$$

The $D_{i,m}$ contain the new concentrations in the form of the non-linear part of Equation 29; therefore, the solution of 33 cannot be obtained directly. As a first approximation, the $D_{i,m}$ can be calculated on the basis of the old concentrations at the end of the kth time interval. Then Equation 33 can be solved by conventional linear techniques for first approximations to the new concentrations. The first approximations can be used, in turn, to calculate improved values of the $D_{i,m}$, and so on. This iterative procedure converges rather rapidly and can be repeated until the desired accuracy is obtained.

Reasonably good solutions can be obtained with the implicit procedure at time intervals two orders of magnitude greater than those required for stability in the backward difference method. The additional computation required for the implicit method, however, reduces the time advantage to approximately a factor of 10.

Evaluation of the Column Coefficients

If it is assumed that the properties of the gas are constant at some average temperature between the hot and cold walls of the column, then relatively simple expressions can be obtained for the three column coefficients, H, K_c and K_d.[12] For conditions of practical interest in gas phase isotope separation, however, the range of temperature across the column annulus is large, and the assumption of constant properties is a poor one.

The most direct way of treating this problem is to construct tables of smoothed experimental properties as functions of temperature. These tables are then used for the numerical integration of the several theoretical equations leading to the column coefficients. Where property data are missing, or of dubious accuracy, they can be calculated, extrapolated and smoothed by use of expressions derived from the kinetic theory of gases[29].

Recent work by Kestin[30], Smith[31] and others[32] has significantly advanced experimental knowledge of gas viscosities over a wide temperature range. Precisely known viscosities can be used to derive parameters for various models of the interatomic potential, and these in turn can be used to calculate the other transport properties of the gas. In the temperature range of practical interest (300 to 1100K) the Lennard-Jones[30], the Dymond-Alder[33,34] and the Klein-Hanley 11-6-8[35,36] potentials

can all be made to fit the available viscosity data. They can be used to calculate the thermal conductivity (for monatomic gases) and the diffusion coefficient with an accuracy sufficient for column calculations. The thermal diffusion factor is less well represented by these potentials; however, the Dymond-Alder potential appears to give the best fit to the most reliable of the experimental data[34].

Recent work by Kestin and coworkers[37,38] on an extended law of corresponding states for the noble gases promises to be of considerable utility in calculating noble gas column transport parameters. The Kestin relationships are successful in predicting the isotopic thermal diffusion factor in addition to the other transport properties.

Shape Factors

According to the kinetic theory of gases the first approximations to the transport properties of a monatomic gas can be written as follows:

$$\eta(T) = \eta(T_R)\theta^{1/2}\Omega^{(2,2)*}(T_R^*)/\Omega^{(2,2)*}(\theta T_R^*) \quad (34)$$

$$\lambda(T) = \lambda(T_R)\theta^{1/2}\Omega^{(2,2)*}(T_R^*)/\Omega^{(2,2)*}(\theta T_R^*); \quad (35)$$

$$D(T) = D(T_R)\theta^{3/2}\Omega^{(1,1)*}(T_R^*)/\Omega^{(1,1)*}(\theta T_R^*); \quad (36)$$

$$\alpha_o(T) = \alpha_o(T_R)[\alpha_o(\theta T_R^*)/\alpha_o(T_R^*)], \quad (37)$$

where $\Omega^{(1,1)*}(T^*)$ and $\Omega^{(2,2)*}(T^*)$ are collision integrals for some specified model of the interatomic potential, and T^* is a reduced temperature defined by

$$T^* = kT/\varepsilon \quad (38)$$

the quantity ε/k is a parameter of the potential model; T_R is a reference temperature, and $\theta = T/T_R$.

If the cold wall temperature of the column, T_2, is chosen as the reference temperature, then the expressions for the column coefficients become

$$H_o = \frac{2\pi g r_2^4}{6!}\left[\frac{\rho^2\alpha_o}{\eta}\right]_{T=T_2} h(T_2^*, \theta_1, y_1), \tag{39}$$

$$K_c = \frac{2\pi g^2 r_2^8}{9!}\left[\frac{\rho^3}{D\eta^2}\right]_{T=T_2} k_c(T_2^*, \theta_1, y_1), \tag{40}$$

$$K_d = 2\pi r_2^2[D\rho]_{T=T_2}\, k_d(T_2^*, \theta_1, y_1), \tag{41}$$

where $y_1 = r_2/r_1$.

The quantities h, k_c and k_d are called shape factors. They are dimensionless functions of the reduced temperature at the cold wall, the ratio of the hot wall temperature to the cold wall temperature and the radius ratio. The shape factors are given by the following expressions derived from Equations 3-5.

$$h = 6!\left[\frac{\ell n y_1}{f(\theta_1)}\right]^3 \int_1^{\theta_1} \frac{\alpha_o(\theta T_2^*)\gamma(\theta)d\theta}{\alpha_o(T_2^*)\quad\theta} \tag{42}$$

$$k_c = 9!\left[\frac{\ell n y_1}{f(\theta_1)}\right]^7 \int_1^{\theta_1} \frac{\Omega^{(1,1)*}(\theta T_2^*)\Omega^{(2,2)}(T_2^*)}{\Omega^{(1,1)*}(T_2^*)\Omega^{(2,2)}(\theta T_2^*)}\gamma^2(\theta)d\theta \tag{43}$$

$$k_d = \left[\frac{\ell n y_1}{f(\theta_1)}\right] \int_1^{\theta_1} \frac{\Omega^{(2,2)*}(T_2^*)\Omega^{(1,1)*}(T_2^*)}{\Omega^{(2,2)*}(\theta T_2^*)\Omega^{(1,1)*}(\theta T_2^*)}\frac{\theta d\theta}{y^2} \tag{44}$$

where the quantity $f(\theta)$ is given by

$$f(\theta) = \int_1^{\theta} \frac{\theta^{1/2}\Omega^{(2,2)*}(T_2^*)}{\Omega^{(2,2)*}(\theta T_2^*)}\, d\theta \tag{45}$$

and

$$\ell n\, y = \frac{f(\theta)}{f(\theta_1)}\, \ell n\, y_1 \tag{46}$$

The quantity $\gamma(\theta)$ is the solution of

$$\frac{d}{d\theta}\frac{\Omega^{(2,2)*}(\theta T_2^*)}{\Omega^{(2,2)*}(T_2^*)}\frac{y^2}{\theta^{1/2}}\frac{d^2}{d\theta^2}\frac{\Omega^{(2,2)*}(\theta T_2^*)}{\Omega^{(2,2)*}(T_2^*)}\, y^2\theta^{1/2}\frac{d\gamma}{d\theta} = \frac{d}{d\theta}\frac{1}{\theta} \tag{47}$$

with boundary conditions

$$\gamma(1) = \gamma(\theta_2) = \left(\frac{d\gamma}{d\theta}\right)_{\theta=1} = \left(\frac{d\gamma}{d\theta}\right)_{\theta=\theta_2} = 0 \cdot \qquad (48)$$

Numerous authors have published tables of shape factors for several models of the intermolecular potential, including the inverse power[39], the Lennard-Jones 12-6,[40] and the modified Buckingham[41]. The tables of Von Halle and coworkers are especially extensive. It should be noted that the shape factors vary quite rapidly in some regions, and conventional interpolation techniques can cause large errors. Accurate results can be obtained by calculating column coefficients for the several table entries surrounding the desired point, then interpolating on the column coefficients.

The author has used shape factors with success in earlier work[14]; however, none of the models for which tabulations are available is adequate to represent the isotopic thermal diffusion factor. The use of carefully selected experimental property values at the cold wall, or reference, temperature can avoid some of the difficulty. Polyatomic gases can be handled only if the thermal conductivity has a temperature dependence similar to that of the molecular force model. (The column coefficients depend only on the temperature variation of the thermal conductivity and not on its absolute value.)

With the widespread availability of digital computer facilities the use of shape factors for calculating column coefficients has become anachronistic. Much better results are obtained by direct integration of the respective expressions based on tables of selected values for each of the physical properties.

III. EXPERIMENTAL EVALUATION OF THERMAL DIFFUSION COLUMN PERFORMANCE

The FJO theory[11] is generally acknowledged to give a qualitatively correct description of the experimental behavior of thermal diffusion columns. Until recently, however, quantitative agreement between separations predicted by the theory and experimentally observed separations was seldom obtained. The poor results were apparently caused by the following factors: 1) failure of the experimental geometry and temperature distribution to match those assumed in the theory; 2) imprecise knowledge of the physical properties of the mixture being separated as functions of temperature; 3) imprecise knowledge of the thermal diffusion factor and its variation with temperature; and 4) experimental data insufficient to allow separate evaluation and comparison of the three coefficients H, K_c, and K_d with theory. The sections which follow will deal with the experimental aspects of this problem, e.g., items 1 and 4.

Column Imperfections

Deviations from the ideal temperature distribution and geometry assumed in the theory lead to parasitic circulation currents in the column. These tend to reduce the separation. In their original review article Jones and Furry[12] attempted to estimate the parasitic effects. For practical gas phase columns it appears that uniformity of temperature is seldom of concern unless a large number of spacers is inserted to establish uniformity of the annular spacing. The performance of the column, however, is very sensitive to deviations from coaxial alignment of the hot and cold walls[42-44]. Experimentally it has been found that poor alignment leads to an apparent increase in the convective remixing coefficient. Thus the total remixing coefficient can be considered to consist of three terms:

$$K = K_d + K_c + K_p \tag{49}$$

where K_p is called the parasitic remixing coefficient and has the same dependence on pressure as does K_c, i.e.,

$$K_p = K_p' p^4 \tag{50}$$

Recently, Sorenson, Willis and Stewart[45] published a theoretical treatment of the parasitic remixing problem. The treatment is based on an orthogonal expansion method, and variable property effects are included. Results predicted from the theory were found to be in good agreement with unpublished experimental data obtained at Mound Laboratory on neon isotope separation in columns having known deviations from ideal geometry. A computer program was provided for general application of the method.

Because of the considerable difficulty associated with defining an imperfect geometry in the laboratory, it is nearly always advantageous in precise experimental work to use great care in designing and fabricating the experimental apparatus. A separate evaluation of the total convective remixing coefficient for a system with well-known physical properties can be used in conjunction with the theory to estimate the magnitude of the residual parasitic effects.

Experimental Evaluation of Column Coefficients

Measurement of the separation factor at total reflux as a function of pressure can be used in conjunction with Equation 13 to derive experimental values of the ratios H'/K_c' and H'/K_d. Frequently a linearized form of Equation 13 is used as the basis for a linear least squares fit of the data:

$$y = ax + b, \tag{51}$$

where $y = Lp^2/\ln q$, $a = K_c'/H'$, $b = K_d/H'$ and $x = p^4$.

This procedure, however, gives much greater weight to data at high pressure, and can lead to apparent error in the evaluation of the intercept, K_d/H'. As the author has shown in Reference 16, the use of a nonlinear fit to Equation 13 avoids the weighting problem.

The diffusive remixing coefficient K_d is independent of the convection process in the column. If the diffusion coefficient of the gas is accurately known as a function of temperature, then the theoretical value of K_d can be used to calculate experimental values of the other two coefficients from total reflux data[16].

If reliable diffusion data cannot be obtained, then additional experiments are required to determine the column transport coefficients. From Equation 2 it is clear that experiments to measure the initial transport coefficient, H, must involve a nonzero value of the transport τ_1. There are two possible approaches: 1) measurement of the separation as a function of time starting from a condition of uniform concentration, or zero separation[46,47]; 2) measurement of the steady state separation in a column operated with a nonzero net flux ($\sigma \neq 0$)[16,17]. Both types of experiments have been reported in the literature. The transient experiment is easier to set up and requires less equipment, but a detailed knowledge of the distribution of the gas holdup in the system is required. The initial transport coefficient is obtained from a solution of the time dependent transport equation with boundary conditions pertaining to the particular holdup distribution of the experimental setup. Sampling errors and cumulative removal of gas from a closed system can be problems in such an experiment.

Method 2 requires measurements of the separation factor as a function of flow rate. For the case of a binary system the

experimental value of H is chosen as that value which gives the best least squares fit to Equation 16. The finite difference solution of Equation 25 is used for a multicomponent system[17]. The flow method is tedious but with proper care and sufficient data, results of better accuracy can be obtained with it.

Over the last decade the author and coworkers completed a systematic evaluation of thermal diffusion column performance and the extent to which it agrees with theoretical predictions [14-20,34,48]. This work covered the following types of isotopic mixtures: 1) binary monatomic gas systems; 2) multicomponent monatomic gas systems; 3) isotopically substituted polyatomic systems; and 4) systems of low atomic or molecular weight. Mixtures of unlike gases were also studied. Precisely constructed and aligned metal columns were used in all of these experiments. Although spacers were used in some of the longer columns to assure coaxial alignment, the distance between spacers was never less than 1.2 m.

Binary Monatomic Gas Systems

The ^{20}Ne-^{22}Ne separation was studied as a function of flow rate, pressure, column geometry and hot wall temperature in an extended series of experiments[16]. Four different column configurations were used ranging in radius ratio (cold wall to hot wall) from 2.95 to 20 and in hot wall temperature from 108 to 815^{0}C. The results of a typical set of total reflux measurements as a function of pressure are shown in Figure 4 and a typical set of data for separation as a function of flow rate is plotted in Figure 5. Theoretical curves for these two figures were recalculated for this review based on physical properties predicted from the generalized Dymond-Alder potential. Parameters for the potential were taken from some of the author's recent work[34].

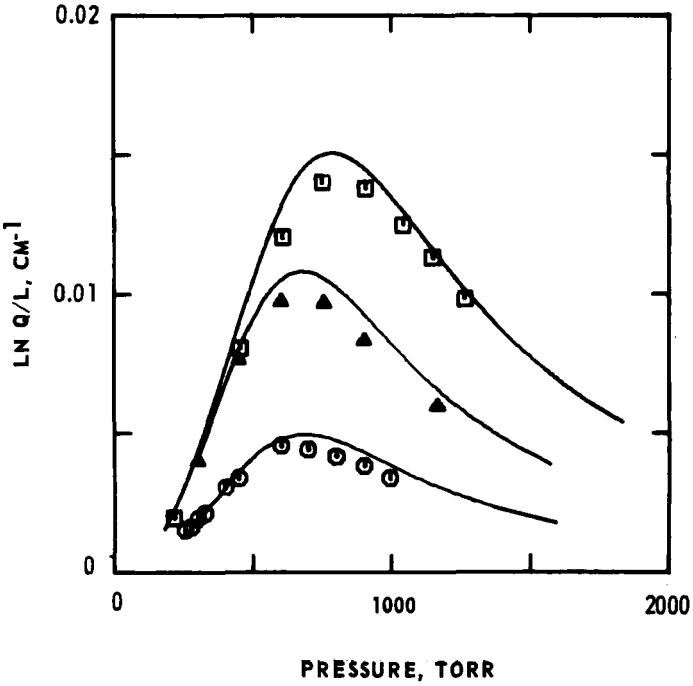

FIGURE 4

Separation of ^{20}Ne-^{22}Ne in column C at total reflux. The experimental parameters were as follows: r_1 = 0.8 mm; r_2 = 9.43 mm; T_2 = 15°C; L = 1.524 m. The solid curves are calculated from theory. The three sets of data are for hot wall temperatures of 200, 500 and 800°C, from bottom to top, respectively.

Tables II and III give experimentally derived values of the column coefficients for the several experimental conditions. As indicated above, the ratios K_d/H' and K_c'/H' were obtained by a nonlinear least squares fit of Equation 13, and H, hence H', was obtained from a similar least squares fit of Equation 16. The theoretical values of the coefficients are those based on the generalized Dymond-Alder potential.

Table IV is a summary of deviations of the coefficients from the values predicted theoretically. It is expressed as

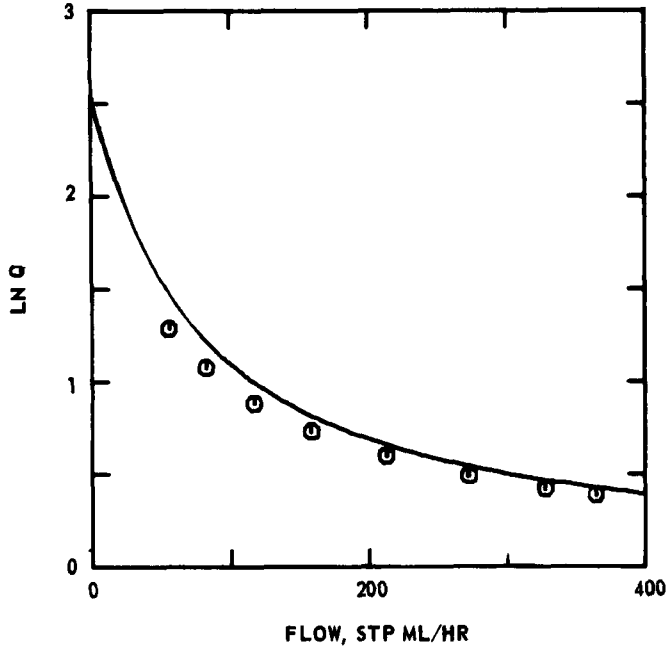

FIGURE 5

Separation of ^{20}Ne-^{22}Ne in column D as a function of flow rate at 1208 torr. The experimental parameters were as follows: $T_1 = 500^0C$; $T_2 = 15^0C$; $r_1 = 3.2$ mm; $r_2 = 9.43$ mm; L = 1.524 m. The solid curve is calculated from theory.

averages of the ratios of the experimental values to the theoretical values for all eight experimental conditions.

The ratios reported in Table IV show that the agreement between theory and experiment is good in spite of the extremely wide range of experimental conditions and thus of the values of the coefficients. Only the ratio for K_c' departs by more than one standard deviation from unity. The quantity reported as K_c' includes parasitic contributions arising from imperfect geometry. As stated previously, the parasitic effects are quite sensitive to these irregularities, and the rather large standard deviation

TABLE II

Reduced Initial Transport Coefficients For ^{20}Ne-^{22}Ne Separation Experiments

Column	r_2/r_1	T_1 (^{0}C)[a]	p(torr)	10 H'(g sec^{-1} atm^{-2}) Measured	Theory
A	20	500	297	32.6	33.6
			497	32.3	
		800	300	42.1	41.7
			553	41.6	
B	16	500	421	13.4	13.2
			706	13.5	
		800	460	16.4	16.0
			810	16.6	
C	11.8	200	765	1.57	1.52
		500	758	3.73	3.92
			1058	3.72	
		800	801	4.23	4.60
			1257	4.29	
D	2.95	108	1262	0.329	0.379
		500	1208	1.63	1.84

[a]The cold wall temperature was 15^{0}C for all experiments.

for these measurements reflects this sensitivity. An apparent low departure of H' from theory, reported in the original paper and ascribed to possible errors in the data available for α_T, is no longer present.

Multicomponent Monatomic Gas Systems

Isotopic separations in the 6-component krypton system[17] and the 9-component xenon system[19] were studied as a function of hot wall temperature, pressure, and flow rate in a single 7.32 m hot wire thermal diffusion column. Hot wall temperatures ranged from 350 to 800^{0}C. Results for measurements at total reflux are given for the ^{80}Kr-^{86}Kr pair in Figure 6 and for the

TABLE III

Remixing Coefficients for ^{20}Ne-^{22}Ne Separation Experiments

Column	T_1 (^0C)	$10^3K_c'$ ($g\ cm\ sec^{-1}\ atm^{-4}$) Measured	Theory	10^3K_d ($g\ cm\ sec^{-1}$) Measured	Theory
A	500	223	210	3.52	4.04
	800	195	147	4.11	4.54
B	500	36.4	29.7	2.49	2.57
	800	23.8	20.0	3.05	2.90
C	200	2.31	1.89	1.27	1.25
	500	2.44	2.28	1.44	1.44
	800	1.32	1.42	1.71	1.64
D	108	0.226	0.162	1.05	1.10
	500	0.259	0.215	1.36	1.43

^{129}Xe-^{136}Xe pair in Figure 7. The separation factor for the ^{80}Kr-^{86}Kr pair as a function of flow rate is plotted in Figure 8 for a hot wall temperature of 800^0C. Separations in both gases were evaluated for each of three isotopic pairs. With allowance for analytical precision it was found that the behavior of each pair was consistent with the mass dependence predicted by the multicomponent transport equation.

TABLE IV

Average Coefficient Ratios for ^{20}Ne-^{22}Ne Separation Experiments

$$H'_{exptl}/H'_{theory} = 0.972 \pm 0.052$$

$$K_c'\ exptl/K_c'\ theory = 1.18 \pm 0.13$$

$$K_d\ exptl/K_d\ theory = 0.973 \pm 0.057$$

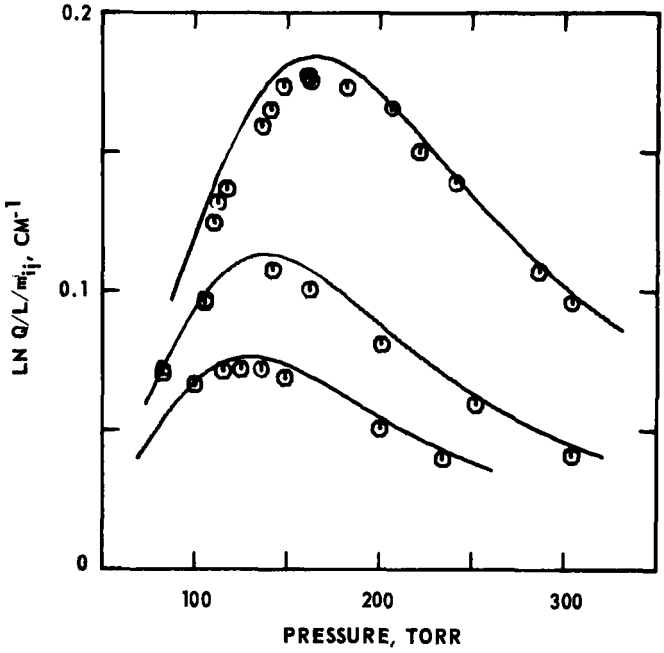

FIGURE 6

Separation of ^{80}Kr-^{86}Kr at total reflux. The experimental parameters were as follows: $T_2 = 15^0C$; $r_1 = 0.795$ mm; $r_2 = 9.525$ mm; L = 4.877 m. The solid curves are calculated from theory. The three sets of data are for hot wall temperatures of 350, 500 and 800^0C, from bottom to top, respectively.

The theoretical curves shown in Figures 6, 7, and 8 were recalculated for this review on the basis of the generalized Dymond-Alder potential function. It was shown in a recent paper[34] that the D-A potential gives a good fit to the isotopic thermal diffusion factors of krypton and xenon in the important low temperature region.

Column coefficients for the multicomponent systems are given in Table V. The ratios K_d/H_o' and K_c'/H_o' were obtained from a nonlinear least squares fit to Equation 26 and H_o' was obtained

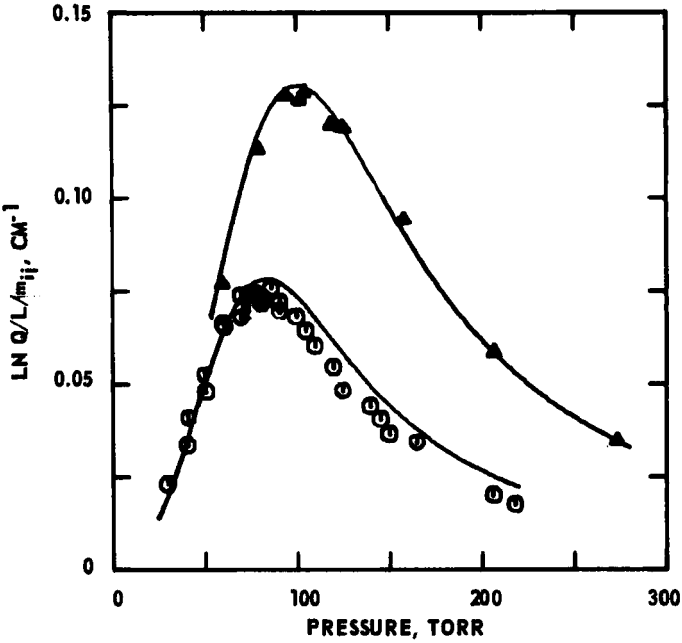

FIGURE 7

Separation of ^{129}Xe-^{136}Xe at total reflux. The experimental parameters were the same as those for Figure 6. The solid curves are calculated from theory. The lower set of data is for $T_1 = 517^0C$ and the upper, for $T_1 = 800^0C$.

by a least squares fit to the finite difference solution of Equation 25. The results reported pertain to the ^{80}Kr-^{86}Kr pair and the ^{129}Xe-^{136}Xe pair. Within the error of the experiments there was no discernible effect of the choice of isotope pair on the experimental results for H'_0.

Table VI gives the composite ratios of the experimental coefficients to those calculated from theory. All three ratios are equal to unity within one standard deviation; thus the experimental results agree with theory within the mutual uncertainty of the measurements and of the theoretical calculations.

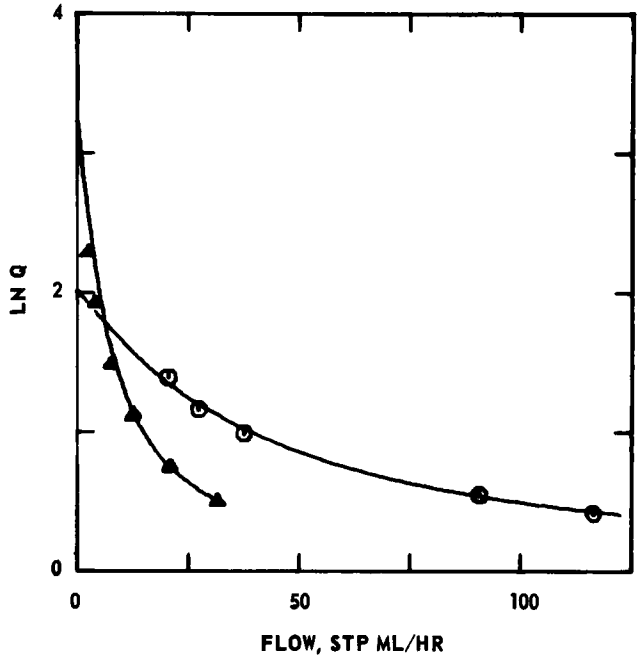

FIGURE 8

Separation of ^{80}Kr-^{86}Kr as a function of flow rate for T_1 = 800°C. The other experimental parameters are the same as those listed for Figure 6. The solid lines are calculated from theory. The triangles are data for p = 158 torr and the circles, for p = 279 torr.

Again, there is evidence of a slight parasitic effect in the positive deviation of the ratio for K_c' from unity.

Isotopically Substituted Polyatomic Systems

Experiments in this series were done on carbon monoxide[14], methane[15], nitrogen and oxygen[18]. These systems were considered to be binary mixtures involving $^{13}C^{16}O$-$^{12}C^{16}O$, $^{13}CH_4$-$^{12}CH_4$, $^{15}N^{14}N$-$^{14}N_2$, and $^{18}O^{16}O$-$^{16}O_2$, respectively. As in the krypton and xenon work, separations were measured as a function of hot wall temperature, pressure and flow rate in a 7.32 m hot wire

TABLE V

Column Coefficients for Kr and Xe Isotope Separation Experiments

	T_1 (°C)[a]	p(Torr)	$10^3 H'_O$ (g sec^{-1} atm^{-2}) Measured	$10^3 H'_O$ (g sec^{-1} atm^{-2}) Theory	K'_C (g cm sec^{-1} atm^{-4}) Measured	K'_C (g cm sec^{-1} atm^{-4}) Theory	$10^3 K_d$ (g cm sec^{-1}) Measured	$10^3 K_d$ (g cm sec^{-1}) Theory
Krypton	350	132	6.33	5.93	1.57	1.33	1.21	1.13
		221	6.87		1.68		1.30	
	500	135	8.27	8.52	1.21	1.14	1.21	1.24
		238	8.48		1.22		1.22	
	800	158	10.56	11.34	0.61	0.657	1.47	1.44
		279	11.65		0.67		1.61	
Xenon	517	83	13.59	15.18	8.50	8.02	1.00	1.17
		147	15.82		9.88		1.16	
	800	102	20.35	20.43	4.36	4.48	1.46	1.37

[a]The cold wall temperature was 15°C for all experiments.

TABLE VI

Average Coefficient Ratios for Kr and Xe
Isotope Separation Experiments

$$(H_o')_{expt1}/(H_o')_{theory} = 1.006 \pm 0.071$$
$$(K_c')_{expt1}/(K_c')_{theory} = 1.088 \pm 0.108$$
$$(K_d)_{expt1}/(K_d)_{theory} = 1.026 \pm 0.083$$

column. Typical sets of total reflux data are shown in Figures 9 and 10 for methane and nitrogen, respectively.

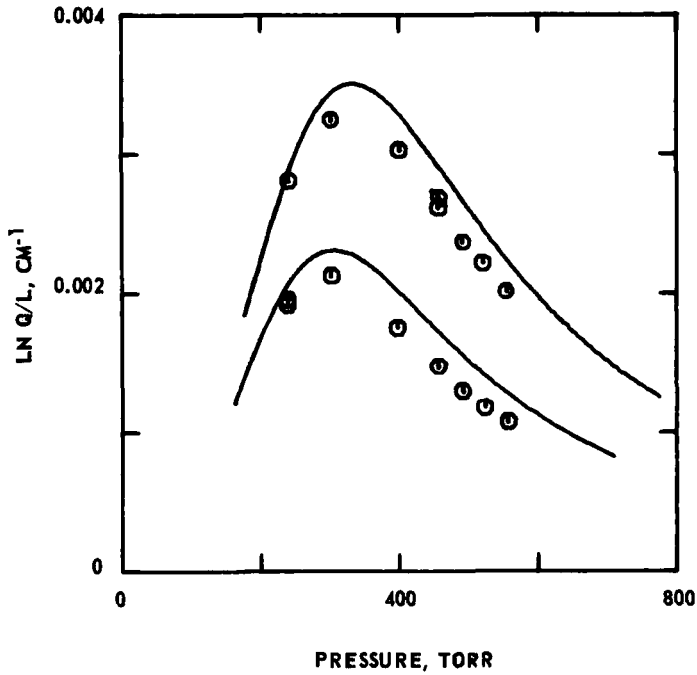

FIGURE 9

Separation of $^{13}CH_4$-$^{12}CH_4$ at total reflux. The experimental parameters were as follows: $T_2 = 15^0C$; $r_1 = 0.795$ mm; $r_2 = 9.525$ mm; $L = 7.315$ m. The solid curves are calculated from theory. The lower set of points is for $T_1 = 320^0C$ and the upper, for 480^0C.

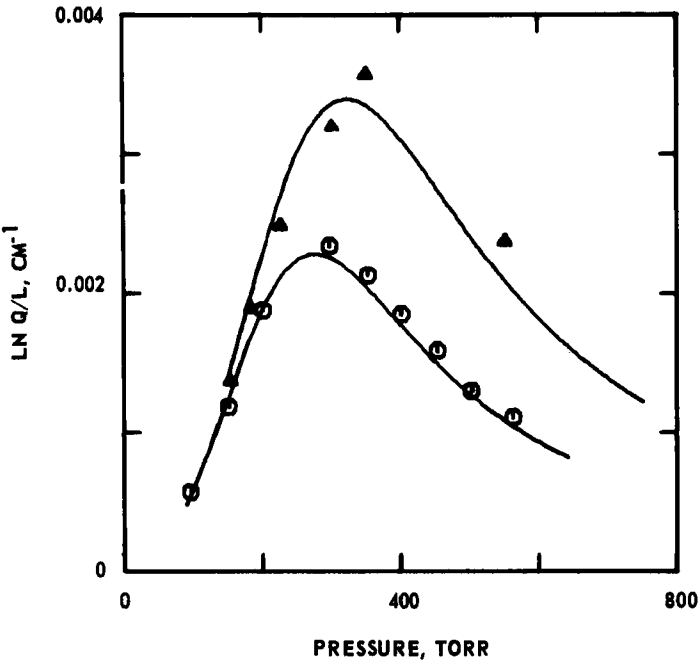

FIGURE 10

Separation of $^{14}N^{15}N$-$^{14}N_2$ at total reflux. The experimental parameters were the same as those given for Figure 9. The lower set of points is for $T_1 = 500^0C$ and the upper, for $T_1 = 800^0C$.

Column coefficients for the polyatomic systems are given in Table VII along with coefficients calculated from theory.

Less information is available on the transport properties of these gases; hence the approach used in the theoretical calculations differs somewhat from that used for the noble gases. Experimental values for the properties of CO at the cold wall temperature were obtained from the literature, and Lennard-Jones shape factors were used to calculate the coefficients. In the case of CH_4 this approach could not be used because the temperature dependence of the thermal conductivity is substantially

TABLE VII

Column Coefficients for Isotopically Substituted Polyatomic Systems

Gas	ε/k(K)	T_1(°C)[a]	$10^5 H'$ (g sec^{-1} atm^{-2}) Measured	$10^5 H'$ (g sec^{-1} atm^{-2}) Theory	$10^2 K'_c$ (g cm sec^{-1} atm^{-4}) Measured	$10^2 K'_c$ (g cm sec^{-1} atm^{-4}) Theory	$10^4 K_d$ (g cm sec^{-1}) Measured	$10^4 K_d$ (g cm sec^{-1}) Theory
CO (mass 28–mass 29)	88	350	2.48	2.40	5.53	5.67	7.17	7.51
		500	3.68	3.26	5.22	5.22	8.64	8.06
CH_4 (mass 16–mass 17)	144	320	1.48	1.54	2.40	2.06	5.23	5.39
		480	2.12	2.16	1.78	1.60	5.88	5.93
N_2 ($^{14}N_2$–$^{14}N^{15}N$)		500	3.29	2.89	5.15	4.78	9.87	8.39
		800	3.58	3.58	2.48	2.91	10.8	9.55
O_2 ($^{16}O_2$–$^{16}O^{18}O$)	134	500	6.24	5.00	5.24	4.56	11.2	10.70
		800	6.84	6.21	2.51	2.66	12.8	12.30

[a]The cold wall temperature was 15°C for all experiments.

different from that predicted on the basis of the Lennard-Jones potential; therefore, the calculation was based on a table of smoothed experimental data for this property. The N_2 and O_2 calculations were based on selected, smoothed tables for all of the transport properties.

For each gas the thermal diffusion factor was taken to be 0.7 times the value predicted on the basis of the Lennard-Jones model. (CO and CH_4 were recalculated using this assumption for this review.) It is a rough approximation, and the justification for using it is based on a limited amount of widely scattered data. The sources of available thermal diffusion data for these systems are cited in the original papers; however, additional measurements on oxygen[49] have appeared since Reference 18 was published.

Average ratios of the experimental column transport coefficients to those calculated from theory are given in Table VIII. There is considerable uncertainty in the theoretical values because of the less satisfactory knowledge of the transport properties; nevertheless, the ratios are quite close to unity--within one standard deviation in each case.

Systems of Low Atomic or Molecular Weight

The FJO theory of the thermal diffusion columns was derived for isotopic mixtures of high atomic or molecular weight; hence,

TABLE VIII

Average Coefficient Ratios for Isotopically Substituted Polyatomic Systems

$$(H')_{exptl}/(H')_{theory} = 1.074 \pm 0.091$$

$$(K_c')_{exptl}/(K_c')_{theory} = 1.034 \pm 0.103$$

$$(K_d)_{exptl}/(K_d)_{theory} = 1.048 \pm 0.072$$

the theory could not be expected to give quantitative results for mixtures of light isotopes such as hydrogen or helium, or for mixtures of unlike gases in general. The theory published by the author in 1970 does not have this restriction, provided that vertical concentration gradients are small[20].

The revised theory was tested in a series of experiments with mixtures of ^{3}He and ^{4}He. The experiments were done in hot wire columns with radius ratios from 16 to 26 and at hot wall temperatures from 320 to 800^{0}C. Mixtures containing high and low concentrations of ^{3}He were used.

Initial transport coefficients were measured by means of flow experiments in short column sections in order to avoid excessive concentration differences across the test section. Thus the column coefficients, which are concentration dependent, could be considered constant in the section. The experimental values of the reduced initial transport coefficient are given in Table IX, along with the average concentrations of ^{3}He.

Concentration profiles were measured at zero flow rate as a function of pressure for each experimental column at each temperature. Several of the profiles are shown in Figure 11, and Figure 12 depicts a typical set of results for the slope $\Delta \ln q/\Delta z$ at the point where the ^{3}He concentration was 50%.

The theoretical results given in Table IX and plotted in Figures 11 and 12 were evaluated using column transport coefficients calculated by direct numerical integration of the appropriate theoretical expressions (Equations 3, 4, 5). The integrations, in turn, were based on smoothed tables of carefully selected transport properties for ^{4}He.

Corrections to the coefficients were made to account for the effect of the ^{3}He concentration on the properties of the gas. The density, of course, is proportional to the average atomic

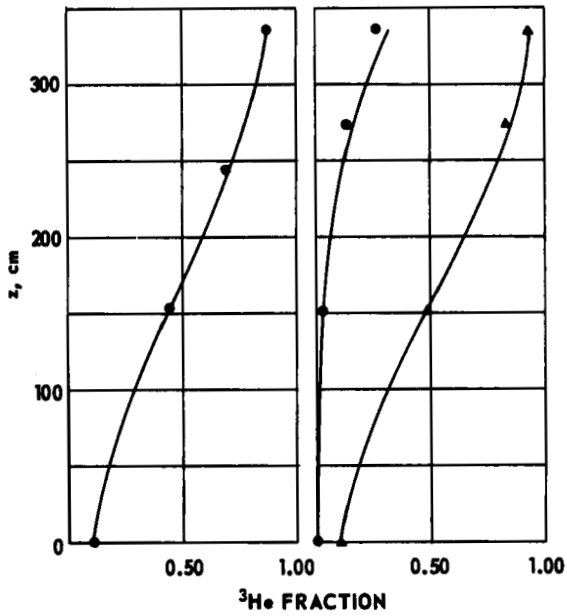

FIGURE 11

Separation of ^3He-^4He at total reflux. Concentration profiles from column 4, T_1 = 800°C, p = 501 torr (data and single curve on the left); and column 2, T_1 = 500°C, p = 1100 torr (data and two curves on the right). The solid lines are calculated from theory.

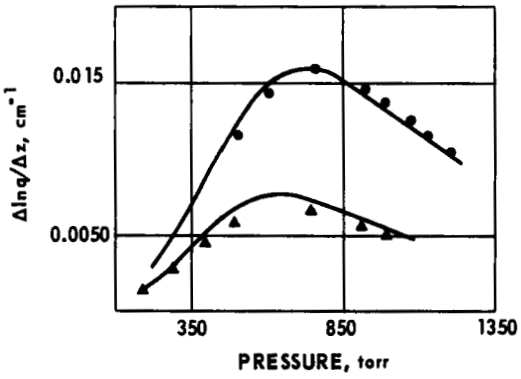

FIGURE 12

Separation of ^3He-^4He at total reflux. The data are for column 4 at T_1 = 320°C (lower set of points) and T_1 = 800°C (upper set of points). The solid curves are calculated from theory.

TABLE IX

The Reduced Initial Transport Coefficient for the Separation of Helium Isotopes

Column	r_2 [b] (cm)	T_1 [a] (^{0}C)	P (torr)	Average ^{3}He Concentration (atom fraction)	$10^5H'$, Exptl. (g sec atm^3)	$10^5H'$, theory
1	1.27	500	1212	0.07	2.30 ± 0.22	2.09
			1942	0.05	2.26 ± 0.38	2.10
2	1.60	500	850	0.35	5.18 ± 0.42	4.76
			1515	0.40	5.37 ± 0.49	4.66
3	1.90	320	776	0.10	7.71 ± 0.79	6.83
			984	0.10	7.53 ± 1.05	6.83
		800	750	0.10	14.05 ± 0.72	13.14
			1200	0.06	14.30 ± 1.07	13.34
4	2.05	320	747	0.08	10.01 ± 1.11	9.27
		800	737	0.03	19.56 ± 1.07	18.40
			1100	0.04	18.62 ± 1.18	18.33
			737	0.85	13.52 ± 0.79	13.02
			1104	0.85	12.67 ± 1.36	13.02

[a]The cold wall temperature was 15^{0}C for all experiments.
[b]The hot wall radius was 0.0795 cm.

weight of the gas, and the viscosity is proportional to the square root of the average atomic weight[29]. The diffusion coefficient, the thermal diffusion factor, and the temperature variation of the thermal conductivity can be assumed to be independent of atomic weight.

The effect of concentration on the column coefficients is shown in Figure 13. Experimental results for the coefficient H at two different ^{3}He concentrations are shown for comparison.

For the ^{3}He-^{4}He experiments the average of the ratios, $(H')_{exptl}/(H')_{theory}$, was found to be 1.074 ± 0.045 and the average of the ratios, $(\ln q)_{exptl}/(\ln q)_{theory}$ was found to be 0.96 ± 0.04. The experimental design did not permit separate experimental evaluations of K'_c and K_d.

Mixtures of Unlike Gases

The modified FJO theory summarized earlier in this paper is applicable to the separation of mixtures of unlike gases, pro-

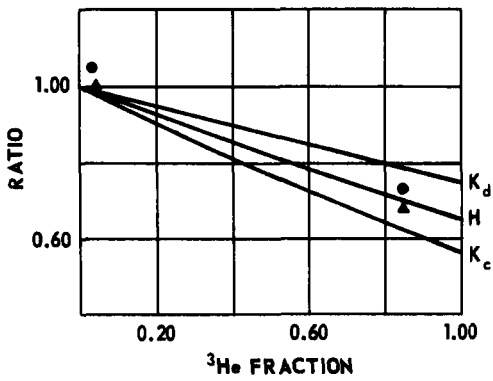

FIGURE 13

Effect of ^{3}He concentration on the column transport coefficients, expressed as ratios of values of the coefficient to those at infinite dilution. The experimental points are derived from measured values of H' for column 4 at $T_1 = 800^0$C. The solid lines are calculated from theory.

vided that the vertical concentration gradient in the column is not excessive. This point was demonstrated by the author by means of separation experiments with dilute neon-xenon mixtures. The experiments were originally designed for measurement of the thermal diffusion factor; however, they can be used equally well to show that separation in this system is accurately predicted by the theory. Figure 14 is a plot of the total reflux separation in this system as a function of pressure at the two extremes of the concentration range. The vertical concentration gradients

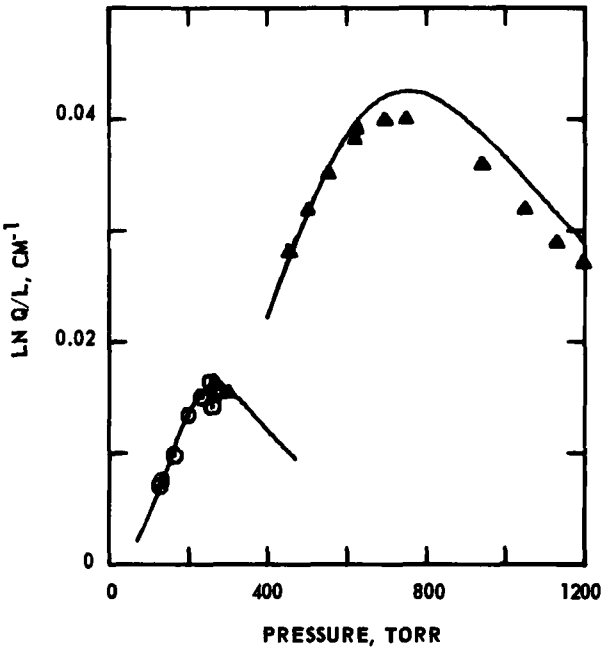

FIGURE 14

Separation of Ne-Xe at total reflux. The lower left curve and points are, for 1 at % Ne, the upper right curve and points are for 98.7% Ne. The experimental parameters were as follows: $T_1 = 75^0C$; $T_2 = 25^0C$; $r_1 = 1.59$ mm; $r_2 = 9.43$ mm; L = 0.914 m (1% Ne); L = 0.457 m (98.7% Ne).

in the experiments were kept small by the use of dilute mixtures and by the use of small temperature differences.

The thermal diffusion factors used to calculate the theoretical curves shown in Figure 14 represent a best fit to the column separation data; however, the values are substantially the same as those of Taylor *et al*[50], obtained by another method.

The ratio K_c'/K_d varied by a factor of approximately 60 over the concentration range from 1.3% Xe to 99% Xe; nevertheless, the experimentally derived value remained within 10% of the value predicted from theory. The experimental values were high, indicating a slight parasitic contribution to K_c'.

IV. CONCLUSIONS

The preceding sections summarize column experiments with nine different gas systems in eight column configurations ranging in cold to hot wall diameter ratio from 3 to 26 and in experimental temperature difference from 50 to 785°C. The range of expected values of the column coefficients was over 2 orders of magnitude for H', over 4 orders of magnitude for K_c' and an order of magnitude for K_d.

There was no evidence of any systematic departure of the experimental results from those expected on the basis of the modified FJO theory of the thermal diffusion column. In several cases minor differences between theory and experiment could be ascribed to small parasitic effects in the apparatus or to imprecise knowledge of the physical properties used in the theoretical calculations. There appears to be no doubt on the basis of this work that the transport coefficients and the separation performance of precisely constructed columns can be predicted from theory within a few percent for conditions normally

considered to be of practical significance in the application of this separation method.

It seems equally clear that the poor results which abound in the thermal diffusion literature are caused by one or more of the following: 1) experimental apparatus which does not conform in geometry and temperature distribution to the assumptions of the theory; 2) end effects in the experiments; 3) the use in the theoretical calculations of inaccurate values of the physical properties of the gas; and 4) the use in the theoretical calculations of inaccurate values of the thermal diffusion factor.

In its present state of development the thermal diffusion column can be used at small temperature differences for the accurate measurement of the thermal diffusion factor. For systems with small thermal diffusion factors the precision of such measurements is equal to or greater than that obtained by other methods such as the swing separator or trennschaukel.

REFERENCES

*Mound Laboratory is operated by Monsanto Research Corporation for the U. S. Energy Research and Development Administration under Contract No. AT-33-1-GEN-53.

1. K. Clusius and G. Dickel, Naturwiss. 26, 546 (1938).
2. B. Th. Verhagen, Proceedings IAEA Symposium on Radioactive Dating and Methods of Low Level Counting, Monaco, March 2-10, 1967, CONF-670309, p. 657.
3. H. von Buttlar and B. Wiik, Proceedings of the Sixth International Conference on Radiocarbon and Tritium Dating, Washington State University, Pullman, Washington, June 7-11, 1965, CONF-650652, p. 515.
4. M. Shimizu and J. Ravoire, CEA Report R-3015, October 1966.
5. W. M. Rutherford, J. Evans and L. A. Currie, in preparation.

6. K. Clusius, J. Chim. Phys. 60, 163 (1963).
7. R. A. Schwind and W. M. Rutherford, Proceedings IAEA Symposium on New Developments in Radiopharmaceuticals and Labelled Compounds, Copenhagen, Denmark, March 26-30, 1973.
8. K. Clusius, M. Huber, H. Hürzeler and E. Schumacher, Z. Naturforsch. 11a, 702 (1956).
9. K. Clusius, E. Schumacher, H. Hürzeler and H. U. Hostettler, Z. Naturforsch. 11a, 709 (1956).
10. W. M. Rutherford, F. W. Weyler and C. F. Eck, Rev. Sci. Instr. 39, 94 (1968).
11. W. H. Furry, R. C. Jones and L. Onsager, Phys. Rev. 55, 1083 (1939).
12. R. C. Jones and W. H. Furry, Revs. Mod. Phys. 18, 151 (1946).
13. S. C. Saxena and S. Raman, Revs. Mod. Phys. 34, 252 (1962).
14. W. M. Rutherford, J. Chem. Phys. 42, 869 (1965).
15. W. M. Rutherford, J. Chem. Phys. 46, 900 (1967).
16. W. M. Rutherford and K. J. Kaminski, J. Chem. Phys. 47, 5427 (1967).
17. W. J. Roos and W. M. Rutherford, J. Chem. Phys. 50, 424 (1969).
18. W. M. Rutherford, W. J. Roos and K. J. Kaminski, J. Chem. Phys. 50, 5359 (1969).
19. W. J. Roos and W. M. Rutherford, J. Chem. Phys. 52, 1684 (1970).
20. W. M. Rutherford, J. Chem. Phys. 53, 4319 (1970).
21. G. R. Grove, USAEC Report MLM-1088, Nov. 14, 1959.
22. E. von Halle, USAEC Report K-1420, June 24, 1959.

23. G. Taniel, CEA Report Bibliography No. 45, 1964, available from Service de Documentation du C.E.A., Centre d'Etudies Nucléaires de Saclay, B. P. No. 2, Gif-sur-Yvette, (S. et O.), France.

24. G. Vasaru, G. Müller, G. Reinhold and T. Fodor, The Thermal Diffusion Column, VEB Deutscher Verlag der Wissenschaften, Berlin, 1969.

25. This definition of G is equivalent to that used in Reference 13 and differs from that of Reference 12.

26. J. Bardeen, Phys. Rev. 57, 35 (1940).

27. J. Bardeen, Phys. Rev. 57, 359A (1940).

28. S. D. Majumdar, Phys. Rev. 81, 844 (1951).

29. J. O. Hirschfelder, C. F. Curtiss and R. B. Bird, Molecular Theory of Gases and Liquids, (Wiley, New York, 1954).

30. J. Kestin, S. T. Ro and W. A. Wakeham, J. Chem. Phys. 56, 4119 (1972).

31. G. C. Maitland and E. B. Smith, Journal of Chemical and Engineering Data 17, 150 (1972).

32. M. Goldblatt and W. E. Wageman, Phys. of Fluids, 14, 1024 (1971) (see also Ref. 31).

33. J. H. Dymond and B. J. Alder, J. Chem. Phys. 51, 309 (1969).

34. W. M. Rutherford, J. Chem. Phys. 58, 1613 (1973).

35. M. Klein and H. J. M. Hanley, J. Chem. Phys. 53, 4722 (1970).

36. H. J. M. Hanley and M. Klein, NBS Technical Note 628, U. S. Department of Commerce, National Bureau of Standards, November 1972.

37. J. Kestin, S. T. Ro and W. Wakeham, Physica 58, 165 (1972).

38. J. M. Hellemans, J. Kestin and S. T. Ro, Physica 71, 1 (1974).

39. E. Greene, R. L. Hoglund and E. von Halle, USAEC Research and Development Report K-1469, Feb. 7, 1966.

40. E. von Halle and R. L. Hoglund, USAEC Research and Development Report K-1679, Dec. 27, 1966.

41. J. M. Savirón, D. González and J. A. Madariaga, Lab.-Rep.-SIE-017, Department of Physics, Sección de Física Experimental del C.S.I.C., Faculty of Sciences, Zaragoza, Spain, Sept. 1965.

42. G. Dickel and A. Bürkholz, Z. Naturforsch. 16a, 760 (1961).

43. S. Raman, S. M. Dave and T. K. S. Narayanan, Phys. Fluids 8, 896 (1965).

44. S. Raman, S. M. Dave and T. K. S. Narayanan, Phys. Fluids 8, 1964 (1965).

45. J. P. Sorenson, M. S. Willis and W. E. Stewart, J. Chem. Phys. 59, 2676 (1973).

46. G. Dickel, K. H. Busen and W. Steiner, Z. Physik. Chem. 17, 1 (1958).

47. P. Szargan and G. Müller, Abh. Dtsch. Akad. Wiss. Berlin, Kl. Chem. Geol. Biol. 7, 233 (1964).

48. W. M. Rutherford, J. Chem. Phys. 54, 4542 (1971).

49. B. P. Mathur and W. W. Watson, J. Chem. Phys. 51, 2210 (1969).

50. W. L. Taylor, S. Weissman, W. J. Haubach and P. T. Pickett, J. Chem. Phys. 50, 4886 (1969).